Invariant Extended Kalman Filtering for Robot Localization using IMU and GPS

Saptadeep Debnath, Anthony Liang, Gaurav Manda, Sunbochen Tang, and Hao Zhou
College of Engineering, University of Michigan, Ann Arbor, MI, USA
{saptadeb,aliangdw,gmanda,tangsun,zhh}@umich.edu

***Abstract*— This paper derives an IMU-GPS-fused inertial navigation observer for a mobile robot using the theory of invariant observer design. One of the main features of invariant observers for invariant systems on Lie groups is that the estimation error is autonomous, hence the observable state variables can be rendered convergent within a domain of attraction that is independent of the system's trajectory. The Invariant Extended Kalman Filter (In-EKF) which is an extension of the Extended Kalman Filter (EKF) is supposed to be more efficient given that the system converges to constant values on a larger set of trajectories as opposed to the equilibrium points that an EKF is based on. This paper explores the implementation of the In-EKF for robot localization and is compared against an implementation of the EKF. The localization is performed on the University of Michigan north campus long-term vision and LIDAR dataset.**

I. INTRODUCTION

Robot localization is the process of determining the pose (*i.e.*, position and orientation) of a mobile robot being given a map. Localization is a fundamental building block for an autonomous robot as the knowledge of where the robot is on the map is essential for decision making about future actions. Accurate estimation of robot pose plays a critical role in a wide range of applications including navigation [1], [2], human motion analysis [3], [4], and machine interaction [5].

Existing approaches to solving robot localization can be broadly classified into two categories, filter based methods and optimization based methods. Optimization based algorithms are often advocated for its superior accuracy but at the cost of intensive computations [6], [7], [8]. Filter based methods like the extended Kalman filter (EKF) based solutions are still extensively used mainly as a result of their efficiency and simplicity [9], [10], [11]. In any filter based sensor fusion framework, estimators are required to achieve convergence to zero of the state estimation error. An emerging methodology to accomplish this goal is the Invariant EKF (In-EKF) built on the symmetry-preserving observer theory [12].

The theory of invariant observer design is based on the estimation error being invariant under the action of a matrix Lie group [13], which has recently led to the development of the Invariant EKF (InEKF) [12], [14], [15] with successful applications and promising results in simultaneous localization and mapping [16] and aided inertial navigation systems [17], [18], [19]. The invariance of the estimation error with respect to a Lie group action is referred to as the symmetries of the system. The main result of the InEKF is that symmetries lead to the estimation error satisfying a "log-linear" autonomous differential equation on the Lie algebra of the corresponding Lie group of system dynamics. Therefore, one can design a nonlinear observer or state estimator with strong convergence within a domain of attraction that is independent of the system's trajectory.

In this article, we derive a left In-EKF for a matrix Lie group, $SE_2(3)$, acting on a navigation system containing an IMU sensor dynamics, and GPS measurements. We show that the defined system satisfies the "group affine" property (log-linear error dynamics) and therefore can be incorporated as the process model of an InEKF. We further discuss inclusion of IMU bias into the observer which is necessary for real-world applications. This work includes the following parts:

- Derivation of a left-invariant EKF for IMU process model with a GPS measurement model;
- State augmentation of the above observer with IMU biases;
- Derivation of a standard EKF for comparison with the LI-EKF;
- Evaluations of the derived observers in a real-world dataset.

The North Campus Long-Term (NCLT) dataset [20] collected here at the University of Michigan is used in this project for experimental evaluation of the derived filters.

The remainder of this article is organized as follows. Background and preliminaries are given in Section II. Section III provides the derivation of a left-invariant EKF for inertial navigation with a left-invariant GPS measurement model. Section IV discusses the state augmentation of the previously derived InEKF with IMU bias. Standard EKF state estimator is described in Section V. Experimental evaluations on the NCLT dataset are presented in Section VI. Finally, Section VII concludes the article and suggests future directions.

EECS 568 Team 16 Final Project Report
[1]YouTube video:
https://youtu.be/aILSsw7K2z8
[2]Project website:
https://team16-mobrob-w20.github.io/inekf-localization
[3]Git Repository:
https://github.com/team16-mobrob-w20/inekf-localization

II. REVIEW OF THEORETICAL BACKGROUND AND PRELIMINARIES

We assume a matrix Lie group [21] denoted $\mathcal{G}$ and its associated Lie Algebra denoted $\mathfrak{g}$. Define

$$\mathcal{L}_{\mathfrak{g}} : \mathbb{R}^{\dim \mathfrak{g}} \to \mathfrak{g}, \tag{1}$$

that takes an element in the tangent space of $\mathcal{G}$ at the identity to its corresponding matrix representation, we can write the exponential map

$$\exp : \mathbb{R}^{\dim \mathfrak{g}} \to \mathcal{G}, \tag{2}$$

that relates a matrix Lie group to its associated Lie algebra as

$$\exp(\boldsymbol{\xi}) = \exp_m(\mathcal{L}_{\mathfrak{g}}(\boldsymbol{\xi})), \tag{3}$$

where $\exp_m(\cdot)$ is the standard matrix exponential.

A process dynamics evolving on the Lie group is denoted by

$$\frac{d}{dt}\mathbf{X}_t = f_{\mathbf{u}_t}(\mathbf{X}_t), \tag{4}$$

where the state $\mathbf{X}_t$ lives in the Lie group $\mathcal{G}$ and $\mathbf{u}_t$ is an input variable. Consider the true state trajectory $\mathbf{X}_t$ and an estimate of it $\bar{\mathbf{X}}_t$. The state estimation error is defined using right or left multiplication of $\mathbf{X}_t^{-1}$ as follows.

Definition 1 (Left and Right Invariant Error [15])**.** *The right- and left-invariant errors between two trajectories $\mathbf{X}_t$ and $\bar{\mathbf{X}}_t$ are:*

$$\boldsymbol{\eta}_t^r = \bar{\mathbf{X}}_t \mathbf{X}_t^{-1} = (\bar{\mathbf{X}}_t \boldsymbol{\Gamma})(\mathbf{X}_t \boldsymbol{\Gamma})^{-1} \quad \textit{(Right-Invariant)} \tag{5}$$

$$\boldsymbol{\eta}_t^l = \mathbf{X}_t^{-1} \bar{\mathbf{X}}_t = (\boldsymbol{\Gamma} \bar{\mathbf{X}}_t)^{-1}(\boldsymbol{\Gamma} \mathbf{X}_t) \quad \textit{(Left-Invariant)}, \tag{6}$$

where $\boldsymbol{\Gamma} \in \mathcal{G}$ is an arbitrary element of the group.

The following two theorems are the fundamental results for deriving an Invariant extended Kalman filter and show that a wide range of nonlinear problems can lead to linear error equations provided the error variable is correctly chosen.

Theorem 1 (Autonomous Error Dynamics [15])**.** *A system is group affine if the dynamics $f_{\mathbf{u}_t}(\cdot)$ satisfies: for all $t > 0$ and $\mathbf{X}_1, \mathbf{X}_2 \in \mathcal{G}$:*

$$f_{\mathbf{u}_t}(\mathbf{X}_1 \mathbf{X}_2) = f_{\mathbf{u}_t}(\mathbf{X}_1)\mathbf{X}_2 + \mathbf{X}_1 f_{\mathbf{u}_t}(\mathbf{X}_2) - \mathbf{X}_1 f_{\mathbf{u}_t}(\mathbf{I}_d)\mathbf{X}_2, \tag{7}$$

where $\mathbf{I}_d$ denotes the identity matrix. Furthermore, if this condition is satisfied, the right- and left-invariant error dynamics are trajectory independent and satisfy:

$$\frac{d}{dt}\boldsymbol{\eta}_t^r = g^r_{\mathbf{u}_t}(\boldsymbol{\eta}_t^r), \textit{ where } g^r_{\mathbf{u}_t}(\boldsymbol{\eta}) = f_{\mathbf{u}_t}(\boldsymbol{\eta}) - \boldsymbol{\eta} f_{\mathbf{u}_t}(\mathbf{I}_d) \tag{8}$$

$$\frac{d}{dt}\boldsymbol{\eta}_t^l = g^l_{\mathbf{u}_t}(\boldsymbol{\eta}_t^l), \textit{ where } g^l_{\mathbf{u}_t}(\boldsymbol{\eta}) = f_{\mathbf{u}_t}(\boldsymbol{\eta}) - f_{\mathbf{u}_t}(\mathbf{I}_d)\boldsymbol{\eta}. \tag{9}$$

Theorem 2 (Log-linear Property of the Error [15])**.** *Consider the right- or left-invariant error $\boldsymbol{\eta}_t^i$ as defined by (5) and (6) between two arbitrarily far trajectories of (4) and (7), the superscript i denoting indifferently l or r. Let $\mathcal{L}_{\mathfrak{g}}$ and $\exp(\cdot)$ be defined as above. Let $\boldsymbol{\xi}_0^i \in \mathbb{R}^{\dim \mathfrak{g}}$ be such that initially*

$$\exp(\boldsymbol{\xi}_0^i) = \boldsymbol{\eta}_0^i. \tag{10}$$

Let $\mathbf{A}_t^i$ be defined by

$$g^i_{\mathbf{u}_t}(\exp(\boldsymbol{\xi})) = \mathcal{L}_{\mathfrak{g}}(\mathbf{A}_t^i \boldsymbol{\xi}) + O(\|\boldsymbol{\xi}\|^2). \tag{11}$$

If $\boldsymbol{\xi}_t^i$ is defined for $t > 0$ by the linear differential equation in $\mathbb{R}^{\dim \mathfrak{g}}$

$$\frac{d}{dt}\boldsymbol{\xi}_t^i = \mathbf{A}_t^i \boldsymbol{\xi}_t^i, \tag{12}$$

then, we have for the true non-linear error $\boldsymbol{\eta}_t^i$, the correspondence at all times and for arbitrarily large errors

$$\forall t \geq 0, \boldsymbol{\eta}_t^i = \exp(\boldsymbol{\xi}_t^i). \tag{13}$$

This theorem states that (12) is not the typical Jacobian linearization along a trajectory because the left- or right-invariant error on the Lie group can be exactly recovered from its solution. This result is of major importance for the propagation (prediction) step of the InEKF.

The adjoint representation plays a key role in the theory of Lie groups and through this linear map we can capture the non-commutative structure of a Lie group.

Definition 2 (The Adjoint Map [21])**.** *Let $\mathcal{G}$ be a matrix Lie group with Lie algebra $\mathfrak{g}$. For any $\mathbf{X} \in \mathcal{G}$, the adjoint map,*

$$Ad_{\mathbf{X}} : \mathfrak{g} \to \mathfrak{g}, \tag{14}$$

is a linear map defined as

$$Ad_{\mathbf{X}}(\mathcal{L}_{\mathfrak{g}}(\boldsymbol{\xi})) = X \mathcal{L}_{\mathfrak{g}}(\boldsymbol{\xi}) X^{-1}. \tag{15}$$

Furthermore, we denote the matrix representation of the adjoint map by $\mathrm{Ad}_{\mathbf{X}}$, such that

$$Ad_{\mathbf{X}}(\mathcal{L}_{\mathfrak{g}}(\boldsymbol{\xi})) = \mathcal{L}_{\mathfrak{g}}(\mathrm{Ad}_{\mathbf{X}}\boldsymbol{\xi}). \tag{16}$$

III. $SE_2(3)$ CONTINUOUS LEFT-INVARIANT EKF

In this section, we derive a Left-Invariant Extended Kalman Filter (LI-EKF) using IMU and GPS measurements. IMU biases are neglected for now to be consistent with the standard InEKF theory. Section IV provides a method for reintroducing the bias terms.

A. State Representation

As with typical aided inertial navigation, we wish to estimate the orientation, velocity, and position of the robot (IMU) in the world frame. These states are represented by $\mathbf{R}_{WB}(t)$, ${}_W\mathbf{v}_{WB}(t)$, and ${}_W\mathbf{p}_{WB}(t)$ respectively. The pose of the IMU, $\{\mathbf{R}_{WB}(t), {}_W\mathbf{p}_{WB}(t)\}$, describes a mapping of a point from sensor frame B to world frame W. The above collection of state variables forms the group of double direct spatial isometry $SE_2(3)$. Specifically, $\mathbf{X}_t \in SE_2(3)$ can be represented by the following matrix:

$$\mathbf{X}_t \triangleq \begin{bmatrix} \mathbf{R}_{WB}(t) & {}_W\mathbf{v}_{WB}(t) & {}_W\mathbf{p}_{WB}(t) \\ \mathbf{0}_{1\times 3} & 1 & 0 \\ \mathbf{0}_{1\times 3} & 0 & 1 \end{bmatrix}. \tag{17}$$

We introduce the following shorthand notation:

$$\mathbf{X}_t \triangleq \begin{bmatrix} \mathbf{R}_t & \mathbf{v}_t & \mathbf{p}_t \\ \mathbf{0}_{1\times 3} & 1 & 0 \\ \mathbf{0}_{1\times 3} & 0 & 1 \end{bmatrix}, \tag{18}$$

$$\mathbf{u}_t \triangleq \begin{bmatrix} {}_B\tilde{\boldsymbol{\omega}}_{WB}(t) \\ {}_B\tilde{\mathbf{a}}_{WB}(t) \end{bmatrix} \triangleq \begin{bmatrix} \boldsymbol{\omega}_t \\ \mathbf{a}_t \end{bmatrix}, \tag{19}$$

where the input $\mathbf{u}_t$ is formed from the angular velocity and linear acceleration measurements coming from the IMU. It is important to note that these measurements are taken in the body (or IMU) frame. State $\mathbf{X}_t$ has a total of 9 degrees of freedom (3 for rotation, 3 for velocity, and 3 for position), indicating the dimension of the associated Lie algebra is also 9. The Lie algebra of $SE_2(3)$, denoted by $\mathfrak{se}_2(3)$, is a 5 dimensional square matrix. Defining a map, $\mathcal{L}_{\mathfrak{g}} : \mathbb{R}^9 \to \mathfrak{g}$, that maps a vector $\boldsymbol{\xi} \in \mathbb{R}^9$ to the corresponding element of the Lie algebram, we can write it as:

$$\mathcal{L}_{\mathfrak{g}}(\boldsymbol{\xi}) = \mathcal{L}_{\mathfrak{g}}\left(\begin{bmatrix} \boldsymbol{\xi}^R \\ \boldsymbol{\xi}^v \\ \boldsymbol{\xi}^p \end{bmatrix}\right) = \begin{bmatrix} \left(\boldsymbol{\xi}^R\right)^\wedge & \boldsymbol{\xi}^v & \boldsymbol{\xi}^p \\ \mathbf{0}_{1\times 3} & 0 & 0 \\ \mathbf{0}_{1\times 3} & 0 & 0 \end{bmatrix}, \quad (20)$$

where $(\cdot)^\wedge$ denotes a 3×3 skew-symmetric matrix.

The exponential mapping is given by the formula:

$$\exp(\boldsymbol{\xi}) = \mathbf{I}_5 + \mathbf{S} + \frac{1-\cos\|\boldsymbol{\xi}\|}{\|\boldsymbol{\xi}\|^2}\mathbf{S}^2 + \frac{\|\boldsymbol{\xi}\| - \sin\|\boldsymbol{\xi}\|}{\|\boldsymbol{\xi}\|^3}\mathbf{S}^3, \quad (21)$$

where $\mathbf{S} = \mathcal{L}_{\mathfrak{g}}(\boldsymbol{\xi})$.

Matrix representation of the adjoint operator is given by:

$$\mathrm{Ad}_{\mathbf{X}_t} = \begin{bmatrix} \mathbf{R}_t & 0 & 0 \\ \mathbf{v}_t \times \mathbf{R}_t & \mathbf{R}_t & 0 \\ \mathbf{p}_t \times \mathbf{R}_t & 0 & \mathbf{R}_t \end{bmatrix}. \quad (22)$$

B. Continuous System Dynamics

The IMU measurements are modeled as being corrupted by additive white Gaussian noise, per

$$\tilde{\boldsymbol{\omega}}_t = \boldsymbol{\omega}_t + \mathbf{w}_t^g, \ \mathbf{w}_t^g \sim \mathcal{GP}(\mathbf{0}_{3\times 1}, \boldsymbol{\Sigma}^g \delta(t-t')) \quad (23)$$

$$\tilde{\mathbf{a}}_t = \mathbf{a}_t + \mathbf{w}_t^a, \ \mathbf{w}_t^a \sim \mathcal{GP}(\mathbf{0}_{3\times 1}, \boldsymbol{\Sigma}^a \delta(t-t')). \quad (24)$$

The IMU dynamics can be written as:

$$\dot{\mathbf{R}}_t = \mathbf{R}_t(\tilde{\boldsymbol{\omega}}_t - \mathbf{w}_t^g)^\wedge \quad (25)$$

$$\dot{\mathbf{v}}_t = \mathbf{R}_t(\tilde{\mathbf{a}}_t - \mathbf{w}_t^a) + \mathbf{g} \quad (26)$$

$$\dot{\mathbf{p}}_t = \mathbf{v}_t, \quad (27)$$

where $\mathbf{g}$ is the gravity vector.

In matrix form, the dynamics can be expressed as

$$\begin{aligned} \frac{d}{dt}\mathbf{X}_t &= \begin{bmatrix} \mathbf{R}_t\tilde{\boldsymbol{\omega}}_t^\wedge & \mathbf{R}_t\tilde{\mathbf{a}}_t + \mathbf{g} & \mathbf{v}_t \\ \mathbf{0}_{1\times 3} & 0 & 0 \\ \mathbf{0}_{1\times 3} & 0 & 0 \end{bmatrix} \\ &\quad - \begin{bmatrix} \mathbf{R}_t & \mathbf{v}_t & \mathbf{p}_t \\ \mathbf{0}_{1\times 3} & 0 & 0 \\ \mathbf{0}_{1\times 3} & 0 & 0 \end{bmatrix} \begin{bmatrix} (\mathbf{w}_t^g)^\wedge & \mathbf{w}_t^a & \mathbf{0}_{3\times 1} \\ \mathbf{0}_{1\times 3} & 0 & 0 \\ \mathbf{0}_{1\times 3} & 0 & 0 \end{bmatrix} \\ &\triangleq f_{\mathbf{u}_t}(\mathbf{X}_t) - \mathbf{X}_t\mathcal{L}_{\mathfrak{g}}(\mathbf{w}_t), \end{aligned} \quad (28)$$

where $\mathbf{w}_t = \left[(\mathbf{w}_t^g)^T, (\mathbf{w}_t^a)^T, \mathbf{0}_{1\times 3}\right]^T$. The deterministic system dynamics, $f_{\mathbf{u}_t}(\cdot)$, can be shown to satisfy the group affine property (7). Therefore, following Theorem 1, the left- and right-invariant error dynamics will evolve independently of the system's state. Elementary computations based on the results of Theorem 1 show that for the noisy model (28) we have

$$\begin{aligned} \frac{d}{dt}\boldsymbol{\eta}_t^l &= f_{\mathbf{u}_t}(\boldsymbol{\eta}_t^l) - f_{\mathbf{u}_t}(\mathbf{I}_d)\boldsymbol{\eta}_t^l + \mathcal{L}_{\mathfrak{g}}(\mathbf{w}_t)\boldsymbol{\eta}_t^l \\ &= g_{\mathbf{u}_t}^l(\boldsymbol{\eta}_t^l) + \mathcal{L}_{\mathfrak{g}}(\mathbf{w}_t)\boldsymbol{\eta}_t^l, \end{aligned} \quad (29)$$

where the second term arises from the additive noise. The derivation follows the results in [15] and is not repeated here.

Theorem 2 furthermore specifies that the invariant error satisfies a log-linear property. Namely, if $\mathbf{A}_t$ is defined by

$$g_{\mathbf{u}_t}^l(\exp(\boldsymbol{\xi})) = \mathcal{L}_{\mathfrak{g}}(\mathbf{A}_t\boldsymbol{\xi}) + O(\|\boldsymbol{\xi}\|^2), \quad (30)$$

then the log of the invariant error, $\boldsymbol{\xi} \in \mathbb{R}^{\dim\mathfrak{g}}$, satisfies the linear system

$$\frac{d}{dt}\boldsymbol{\xi}_t = \mathbf{A}_t\boldsymbol{\xi}_t + \mathbf{w}_t. \quad (31)$$

We provide a quick proof of (31) below, from (29),

$$\begin{aligned} \frac{d}{dt}\boldsymbol{\eta}_t &= \frac{d}{dt}\exp(\boldsymbol{\xi}_t) \approx \frac{d}{dt}\left(\mathbf{I}_d + \mathcal{L}_{\mathfrak{g}}(\boldsymbol{\xi}_t)\right) = \frac{d}{dt}\left(\mathcal{L}_{\mathfrak{g}}(\boldsymbol{\xi}_t)\right) \\ &= g_{\mathbf{u}_t}^l\left(\exp(\boldsymbol{\xi}_t)\right) + \mathcal{L}_{\mathfrak{g}}(\mathbf{w}_t)\exp(\boldsymbol{\xi}_t) \\ &\approx \mathcal{L}_{\mathfrak{g}}(\mathbf{A}_t\boldsymbol{\xi}_t) + O(\|\boldsymbol{\xi}_t\|^2) + \mathcal{L}_{\mathfrak{g}}(\mathbf{w}_t)\left(\mathbf{I}_d + \mathcal{L}_{\mathfrak{g}}(\boldsymbol{\xi}_t)\right) \\ &= \mathcal{L}_{\mathfrak{g}}\left(\mathbf{A}_t\boldsymbol{\xi}_t + \mathbf{w}_t\right) + O(\|\boldsymbol{\xi}_t\|^2) + O(\|\mathbf{w}_t\|\|\boldsymbol{\xi}_t\|), \\ &\implies \frac{d}{dt}\left(\mathcal{L}_{\mathfrak{g}}(\boldsymbol{\xi}_t)\right) = \mathcal{L}_{\mathfrak{g}}\left(\mathbf{A}_t\boldsymbol{\xi}_t + \mathbf{w}_t\right), \\ &\implies \frac{d}{dt}\boldsymbol{\xi}_t = \mathbf{A}_t\boldsymbol{\xi}_t + \mathbf{w}_t. \end{aligned} \quad (32)$$

To compute the matrix $\mathbf{A}_t$, we linearize the invariant error dynamics, $g_{\mathbf{u}_t}^l(\cdot)$, using the first order approximation

$$\boldsymbol{\eta}_t^l = \exp(\boldsymbol{\xi}_t) \approx \mathbf{I}_d + \mathcal{L}_{\mathfrak{g}}(\boldsymbol{\xi}_t), \quad (33)$$

to yield

$$\begin{aligned} g_{\mathbf{u}_t}^l(\boldsymbol{\eta}_t^l) &= g_{\mathbf{u}_t}^l\left(\mathbf{I}_d + \mathcal{L}_{\mathfrak{g}}(\boldsymbol{\xi}_t)\right) \\ &= f_{\mathbf{u}_t}\left(\mathbf{I}_d + \mathcal{L}_{\mathfrak{g}}(\boldsymbol{\xi}_t)\right) - f_{\mathbf{u}_t}(\mathbf{I}_d)\left(\mathbf{I}_d + \mathcal{L}_{\mathfrak{g}}(\boldsymbol{\xi}_t)\right) \\ &= \begin{bmatrix} \left(\mathbf{I} + \left(\boldsymbol{\xi}_t^R\right)^\wedge\right)\tilde{\boldsymbol{\omega}}_t^\wedge & \left(\mathbf{I} + \left(\boldsymbol{\xi}_t^R\right)^\wedge\right)\tilde{\mathbf{a}}_t + \mathbf{g} & \boldsymbol{\xi}_t^v \\ \mathbf{0}_{1\times 3} & 0 & 0 \\ \mathbf{0}_{1\times 3} & 0 & 0 \end{bmatrix} \\ &\quad - \begin{bmatrix} \tilde{\boldsymbol{\omega}}_t^\wedge & \tilde{\mathbf{a}}_t + \mathbf{g} & \mathbf{0}_{3,1} \\ \mathbf{0}_{1\times 3} & 0 & 0 \\ \mathbf{0}_{1\times 3} & 0 & 0 \end{bmatrix} \begin{bmatrix} \mathbf{I} + \left(\boldsymbol{\xi}_t^R\right)^\wedge & \boldsymbol{\xi}_t^v & \boldsymbol{\xi}_t^p \\ \mathbf{0}_{1\times 3} & 1 & 0 \\ \mathbf{0}_{1\times 3} & 0 & 1 \end{bmatrix} \\ &= \begin{bmatrix} G_{11} & G_{12} & G_{13} \\ \mathbf{0}_{1\times 3} & 0 & 0 \\ \mathbf{0}_{1\times 3} & 0 & 0 \end{bmatrix}, \end{aligned}$$

where $\mathbf{I} = \mathbf{I}_{3\times 3}$,

$$\begin{aligned} G_{11} &= \left(\boldsymbol{\xi}_t^R\right)^\wedge\tilde{\boldsymbol{\omega}}_t^\wedge - \tilde{\boldsymbol{\omega}}_t^\wedge\left(\boldsymbol{\xi}_t^R\right)^\wedge = \left(-\tilde{\boldsymbol{\omega}}_t^\wedge\boldsymbol{\xi}_t^R\right)^\wedge, \\ G_{12} &= \left(\boldsymbol{\xi}_t^R\right)^\wedge\tilde{\mathbf{a}}_t - \tilde{\boldsymbol{\omega}}_t^\wedge\boldsymbol{\xi}_t^v, \\ G_{13} &= \boldsymbol{\xi}_t^v - \tilde{\boldsymbol{\omega}}_t^\wedge\boldsymbol{\xi}_t^p. \end{aligned} \quad (34)$$

We can further write $g^l_{\mathbf{u}_t}(\cdot)$ as

$$
\begin{aligned}
g^l_{\mathbf{u}_t}(\boldsymbol{\eta}^l_t) &= \begin{bmatrix} G_{11} & G_{12} & G_{13} \\ \mathbf{0}_{1\times 3} & 0 & 0 \\ \mathbf{0}_{1\times 3} & 0 & 0 \end{bmatrix} \\
&= \mathcal{L}_{\mathfrak{g}}\left(\begin{bmatrix} -\tilde{\boldsymbol{\omega}}^{\wedge}_t \boldsymbol{\xi}^R_t \\ -\tilde{\mathbf{a}}^{\wedge}_t \boldsymbol{\xi}^R_t - \tilde{\boldsymbol{\omega}}^{\wedge}_t \boldsymbol{\xi}^v_t \\ \boldsymbol{\xi}^v_t - \tilde{\boldsymbol{\omega}}^{\wedge}_t \boldsymbol{\xi}^p_t \end{bmatrix}\right) \\
&= \mathcal{L}_{\mathfrak{g}}\left(\begin{bmatrix} -\tilde{\boldsymbol{\omega}}^{\wedge}_t & \mathbf{0}_{3\times 3} & \mathbf{0}_{3\times 3} \\ -\tilde{\mathbf{a}}^{\wedge}_t & -\tilde{\boldsymbol{\omega}}^{\wedge}_t & \mathbf{0}_{3\times 3} \\ \mathbf{0}_{3\times 3} & \mathbf{I}_{3\times 3} & -\tilde{\boldsymbol{\omega}}^{\wedge}_t \end{bmatrix} \begin{bmatrix} \boldsymbol{\xi}^R_t \\ \boldsymbol{\xi}^v_t \\ \boldsymbol{\xi}^p_t \end{bmatrix}\right). \quad (35)
\end{aligned}
$$

With the above, we can express the prediction step of the LI-EKF. The state estimate, $\hat{\mathbf{X}}_t$, is propagated though the deterministic system dynamics, while the covariance matrix, $\mathbf{P}_t$, is computed using the Riccati equation, namely,

$$
\frac{d}{dt}\hat{\mathbf{X}}_t = f_{\mathbf{u}_t}(\hat{\mathbf{X}}_t), \frac{d}{dt}\mathbf{P}_t = \mathbf{A}_t\mathbf{P}_t + \mathbf{P}_t\mathbf{A}_t + \hat{\mathbf{Q}}_t, \quad (36)
$$

where the matrices $\mathbf{A}_t$ and $\hat{\mathbf{Q}}_t$ are obtained from (35) and (31),

$$
\mathbf{A}_t = \begin{bmatrix} -\tilde{\boldsymbol{\omega}}^{\wedge}_t & \mathbf{0}_{3\times 3} & \mathbf{0}_{3\times 3} \\ -\tilde{\mathbf{a}}^{\wedge}_t & -\tilde{\boldsymbol{\omega}}^{\wedge}_t & \mathbf{0}_{3\times 3} \\ \mathbf{0}_{3\times 3} & \mathbf{I}_{3\times 3} & -\tilde{\boldsymbol{\omega}}^{\wedge}_t \end{bmatrix}, \hat{\mathbf{Q}}_t = \mathrm{Cov}[\mathbf{w}_t]. \quad (37)
$$

C. Discretization

The continuous dynamics can be discretized by assuming a zero-order hold on the inputs and performing Euler integration from t_{k-1} to t_k. The discrete dynamics for the individual state elements becomes:

$$
\begin{aligned}
\hat{\mathbf{R}}_{t_k} &= \mathbf{R}_{t_{k-1}}\exp(\tilde{\boldsymbol{\omega}}_t\Delta t) && (38)\\
\hat{\mathbf{v}}_{t_k} &= \mathbf{v}_{t_{k-1}} + (\mathbf{R}_{t_{k-1}}\tilde{\mathbf{a}}_t + \mathbf{g})\Delta t && (39)\\
\hat{\mathbf{p}}_{t_k} &= \mathbf{p}_{t_{k-1}} + \mathbf{v}_{t_{k-1}}\Delta t + \frac{1}{2}(\mathbf{R}_{t_{k-1}}\tilde{\mathbf{a}}_t + \mathbf{g})\Delta t^2, && (40)
\end{aligned}
$$

where $\Delta t = t_k - t_{k-1}$ and $\exp(\cdot)$ is the exponential map for $SO(3)$. A first-order approximation can be used to simplify integration of the Riccati equation, resulting in the following discrete-time covariance propagation equation,

$$
\mathbf{P}_k = \boldsymbol{\Phi}\mathbf{P}_{k-1}\boldsymbol{\Phi}^T + \hat{\mathbf{Q}}_{k-1}, \quad (41)
$$

where

$$
\begin{aligned}
\boldsymbol{\Phi} &= \exp_m(\mathbf{A}_t\Delta t) && (42)\\
\hat{\mathbf{Q}}_{k-1} &\approx \boldsymbol{\Phi}\hat{\mathbf{Q}}_t\boldsymbol{\Phi}^T\Delta t. && (43)
\end{aligned}
$$

D. Left-invariant Measurement Model

The GPS measurement model corresponds to the left-invariant observation form: $\mathbf{Y}_{t_k} = \hat{\mathbf{X}}_{t_k}\mathbf{b} + \mathbf{V}_{t_k}$,

$$
\begin{bmatrix} \mathbf{y}_{t_k} \\ 0 \\ 1 \end{bmatrix} = \begin{bmatrix} \hat{\mathbf{R}}_{t_k} & \hat{\mathbf{v}}_{t_k} & \hat{\mathbf{p}}_{t_k} \\ \mathbf{0}_{1\times 3} & 1 & 0 \\ \mathbf{0}_{1\times 3} & 0 & 1 \end{bmatrix} \begin{bmatrix} \mathbf{0}_{3\times 1} \\ 0 \\ 1 \end{bmatrix} + \begin{bmatrix} \mathbf{v}_{t_k} \\ 0 \\ 0 \end{bmatrix} \quad (44)
$$

Therefore, the innovation depends solely on the invariant error and the update equations take the form

$$
\hat{\mathbf{X}}^+_{t_k} = \hat{\mathbf{X}}_{t_k}\exp\left(\mathbf{L}_{t_k}\left(\hat{\mathbf{X}}^{-1}_{t_k}\mathbf{Y}_{t_k} - \mathbf{b}\right)\right) \quad (45)
$$

$$
\boldsymbol{\eta}^{l+}_{t_k} = \boldsymbol{\eta}^l_{t_k}\exp\left(\mathbf{L}_{t_k}\left(\left(\boldsymbol{\eta}^l_{t_k}\right)^{-1}\mathbf{b} - \mathbf{b} + \hat{\mathbf{X}}^{-1}_{t_k}\mathbf{V}_{t_k}\right)\right) \quad (46)
$$

where $\exp(\cdot)$ is the exponential map corresponding to the state matrix Lie group, $\mathbf{L}_{t_k}$ is a gain matrix to be defined later. Linearizing the left-invariant error $\boldsymbol{\eta}^l_{t_k}$ and neglecting the higher order terms, we get

$$
{\boldsymbol{\xi}^l_{t_k}}^+ = \boldsymbol{\xi}^l_{t_k} + \mathbf{L}_{t_k}(-\mathcal{L}_{\mathfrak{g}}(\boldsymbol{\xi}^l_{t_k})\mathbf{b} + \hat{\mathbf{X}}^{-1}_{t_k}\mathbf{V}_{t_k}) \quad (47)
$$

Define the measurement Jacobian, $\mathbf{H}$, such that

$$
\begin{aligned}
\mathbf{H}\boldsymbol{\xi} = \mathcal{L}_{\mathfrak{g}}(\boldsymbol{\xi})\mathbf{b} &= \begin{bmatrix} \left(\boldsymbol{\xi}^R\right)^{\wedge} & \boldsymbol{\xi}^v & \boldsymbol{\xi}^p \\ \mathbf{0}_{1\times 3} & 0 & 0 \\ \mathbf{0}_{1\times 3} & 0 & 0 \end{bmatrix} \begin{bmatrix} \mathbf{0}_{3\times 1} \\ 0 \\ 1 \end{bmatrix} \\
&= \begin{bmatrix} \boldsymbol{\xi}^p \\ 0 \\ 0 \end{bmatrix} = \begin{bmatrix} \mathbf{0}_{3\times 3} & \mathbf{0}_{3\times 3} & \mathbf{I}_{3\times 3} \\ \mathbf{0}_{1\times 3} & 0 & 0 \\ \mathbf{0}_{1\times 3} & 0 & 0 \end{bmatrix} \begin{bmatrix} \boldsymbol{\xi}^R \\ \boldsymbol{\xi}^v \\ \boldsymbol{\xi}^p \end{bmatrix}, \quad (48)
\end{aligned}
$$

and in its reduced form,

$$
\mathbf{H} = \begin{bmatrix} \mathbf{0}_{3\times 3} & \mathbf{0}_{3\times 3} & \mathbf{I}_{3\times 3} \end{bmatrix}. \quad (49)
$$

We can further write the linearized error as

$$
\begin{aligned}
\boldsymbol{\xi}^{l+}_{t_k} &= \boldsymbol{\xi}^l_{t_k} - \mathbf{L}_{t_k}\mathbf{H}\boldsymbol{\xi}^l_{t_k} + \mathbf{L}_{t_k}\hat{\mathbf{X}}^{-1}_{t_k}\mathbf{V}_{t_k} && (50)\\
&= (\mathbf{I} - \mathbf{L}_{t_k}\mathbf{H})\boldsymbol{\xi}^l_{t_k} + \mathbf{L}_{t_k}\hat{\mathbf{X}}^{-1}_{t_k}\mathbf{V}_{t_k} && (51)
\end{aligned}
$$

Finally, we can write down the full state and covariance update equations of the LI-EKF using the derived linear update equation and the theory of Kalman filtering as

$$
\hat{\mathbf{X}}^+_{t_k} = \hat{\mathbf{X}}_{t_k}\exp\left(\mathbf{L}_{t_k}\left(\hat{\mathbf{X}}^{-1}_{t_k}\mathbf{Y}_{t_k} - \mathbf{b}\right)\right) \quad (52)
$$

$$
\mathbf{P}^+_{t_k} = (\mathbf{I} - \mathbf{L}_{t_k}\mathbf{H})\mathbf{P}_{t_k}(\mathbf{I} - \mathbf{L}_{t_k}\mathbf{H})^T + \mathbf{L}_{t_k}\hat{\mathbf{N}}_{t_k}\mathbf{L}^T_{t_k}, \quad (53)
$$

where

$$
\begin{aligned}
\hat{\mathbf{N}}_{t_k} &= \hat{\mathbf{X}}^{-1}_{t_k}\mathrm{Cov}[\mathbf{V}_{t_k}]\hat{\mathbf{X}}^{-T}_{t_k}, && (54)\\
\mathbf{L}_{t_k} &= \mathbf{P}_{t_k}\mathbf{H}^T\mathbf{S}^{-1}, && (55)\\
\mathbf{S} &= \mathbf{H}\mathbf{P}_{t_k}\mathbf{H}^T + \hat{\mathbf{N}}_{t_k}. && (56)
\end{aligned}
$$

IV. INCLUDING IMU BIASES

Our previous discussion is based on IMU measurements modeled with additive white Gaussian noise. In practice, especially in guidance applications where accelerations are constantly being integrated to calculate velocity and position ("dead reckoning"), IMU measurements could be corrupted by an error accumulated over time. To include such accumulated error, also referred to as IMU biases, additional states such as accelerometer biases are typically modeled. Unfortunately, the bias dynamics cannot be incorporated into a Lie group with previously defined states while the group affine property is maintained. In this section, following Manni's work [18], [19], we attempt to design an "Imperfect InEKF", which treats the additional bias states outside Lie group, and evaluate its performance.

A. State Representation

Considering the IMU biases, the IMU measurement model is now rewritten as:

$$\tilde{\boldsymbol{\omega}}_t = \boldsymbol{\omega}_t + \mathbf{b}_t^g + \mathbf{w}_t^g,\ \mathbf{w}_t^g \sim \mathcal{GP}(\mathbf{0}_{3\times1}, \boldsymbol{\Sigma}^g \delta(t-t'))$$
$$\tilde{\mathbf{a}}_t = \mathbf{a}_t + \mathbf{b}_t^a + \mathbf{w}_t^a,\ \mathbf{w}_t^a \sim \mathcal{GP}(\mathbf{0}_{3\times1}, \boldsymbol{\Sigma}^a \delta(t-t')).$$

We now define a parameter vector for these biases which needs to be accurately estimated,

$$\boldsymbol{\theta}_t \triangleq \begin{bmatrix}\mathbf{b}^g(t)\\ \mathbf{b}^a(t)\end{bmatrix} \triangleq \begin{bmatrix}\mathbf{b}_t^g\\ \mathbf{b}_t^a\end{bmatrix} \in \mathbb{R}^6. \tag{57}$$

Incorporating the bias parameter into the LI-EKF state, the new model's state is now a tuple of previously defined state in Lie group and the parameter vector, $(\mathbf{X}_t, \boldsymbol{\theta}_t) \in \mathcal{G} \times \mathbb{R}^6$. The left-invariant error is rewritten as,

$$\mathbf{e}_t^l \triangleq (\mathbf{X}_t^{-1}\hat{\mathbf{X}}_t, \hat{\boldsymbol{\theta}}_t - \boldsymbol{\theta}_t) \triangleq (\boldsymbol{\eta}_t^l, \boldsymbol{\zeta}_t). \tag{58}$$

B. Continuous-time dynamics

The left invariant error of Lie group state $\boldsymbol{\eta}_t^l$ can be written explicitly as:

$$\begin{aligned}\boldsymbol{\eta}_t^l &= \mathbf{X}_t^{-1}\hat{\mathbf{X}}_t\\ &= \begin{bmatrix}\mathbf{R}_t^{-1} & -\mathbf{R}_t^{-1}\mathbf{v}_t & -\mathbf{R}_t^{-1}\mathbf{p}_t\\ \mathbf{0}_{1\times3} & 1 & 0\\ \mathbf{0}_{1\times3} & 0 & 1\end{bmatrix}\begin{bmatrix}\hat{\mathbf{R}}_t & \hat{\mathbf{v}}_t & \hat{\mathbf{p}}_t\\ \mathbf{0}_{1\times3} & 1 & 0\\ \mathbf{0}_{1\times3} & 0 & 1\end{bmatrix}\\ &= \begin{bmatrix}\mathbf{R}_t^{-1}\hat{\mathbf{R}}_t & \mathbf{R}_t^{-1}\hat{\mathbf{v}}_t - \mathbf{R}_t^{-1}\mathbf{v}_t & \mathbf{R}_t^{-1}\hat{\mathbf{p}}_t - \mathbf{R}_t^{-1}\mathbf{p}_t\\ \mathbf{0}_{1\times3} & 1 & 0\\ \mathbf{0}_{1\times3} & 0 & 1\end{bmatrix},\end{aligned}$$

while the parameter vector error is given by

$$\boldsymbol{\zeta}_t \triangleq \begin{bmatrix}\hat{\mathbf{b}}_t^g - \mathbf{b}_t^g\\ \hat{\mathbf{b}}_t^a - \mathbf{b}_t^a\end{bmatrix} \triangleq \begin{bmatrix}\boldsymbol{\zeta}_t^g\\ \boldsymbol{\zeta}_t^a.\end{bmatrix}$$

With the IMU measurement model now including bias, the IMU dynamics can be rewritten as:

$$\begin{aligned}\dot{\mathbf{R}}_t &= \mathbf{R}_t(\tilde{\boldsymbol{\omega}}_t - \mathbf{b}_t^g - \mathbf{w}_t^g)^\wedge\\ \dot{\mathbf{v}}_t &= \mathbf{R}_t(\tilde{\mathbf{a}}_t - \mathbf{b}_t^a - \mathbf{w}_t^a) + \mathbf{g}\\ \dot{\mathbf{p}}_t &= \mathbf{v}_t.\end{aligned}$$

The IMU bias dynamics are modeled using the typical "Brownian motion" model, i.e., the derivatives are white Gaussian noise,

$$\dot{\mathbf{b}}_t^g = \mathbf{w}_t^{bg},\ \mathbf{w}_t^{bg} \sim \mathcal{GP}(\mathbf{0}_{3\times1}, \boldsymbol{\Sigma}^{bg}\delta(t-t'))$$
$$\dot{\mathbf{b}}_t^a = \mathbf{w}_t^{ba},\ \mathbf{w}_t^{ba} \sim \mathcal{GP}(\mathbf{0}_{3\times1}, \boldsymbol{\Sigma}^{ba}\delta(t-t')).$$

The deterministic system dynamics now becomes

$$f_{\mathbf{u}_t,\theta_t}(\mathbf{X}_t, \boldsymbol{\theta}_t) = \begin{bmatrix}\mathbf{R}_t\bar{\boldsymbol{\omega}}_t^\wedge & \mathbf{R}_t\bar{\mathbf{a}}_t + \mathbf{g} & \mathbf{v}_t\\ \mathbf{0}_{1\times3} & 0 & 0\\ \mathbf{0}_{1\times3} & 0 & 0\end{bmatrix}, \tag{59}$$

where

$$\bar{\boldsymbol{\omega}}_t \triangleq \tilde{\boldsymbol{\omega}}_t - \mathbf{b}_t^g \tag{60}$$
$$\bar{\mathbf{a}}_t \triangleq \tilde{\mathbf{a}}_t - \mathbf{a}_t^g, \tag{61}$$

are the "bias-corrected" inputs. To compute the linearized error dynamics, the augmented left-invariant error (58) is first differentiated with respect to time,

$$\dot{\mathbf{e}}_t^l = \left(\dot{\boldsymbol{\eta}}_t^l, \begin{bmatrix}\mathbf{w}_t^{bg}\\ \mathbf{w}_t^{ba}\end{bmatrix}\right). \tag{62}$$

It follows from chain rule and first order approximation $\boldsymbol{\eta}_t^l = \mathbf{I}_d + (\boldsymbol{\xi}_t^l)^\wedge$ that,

$$\begin{aligned}\frac{d}{dt}\left(\mathbf{R}_t^{-1}\hat{\mathbf{R}}_t\right) &= \left(\frac{d}{dt}\mathbf{R}_t\right)^T\hat{\mathbf{R}}_t + \mathbf{R}_t^T\left(\frac{d}{dt}\hat{\mathbf{R}}_t\right)\\ &= (\mathbf{R}_t(\tilde{\boldsymbol{\omega}}_t - \mathbf{b}_t^g - \mathbf{w}_t^g)^\wedge)^T\hat{\mathbf{R}}_t + \mathbf{R}_t^T\hat{\mathbf{R}}_t(\tilde{\boldsymbol{\omega}}_t - \hat{\mathbf{b}}_t^g)^\wedge\\ &= -(\tilde{\boldsymbol{\omega}}_t - \mathbf{b}_t^g - \mathbf{w}_t^g)^\wedge\mathbf{R}_t^T\hat{\mathbf{R}}_t + \mathbf{R}_t^T\hat{\mathbf{R}}_t(\tilde{\boldsymbol{\omega}}_t - \hat{\mathbf{b}}_t^g)^\wedge\\ &\approx -(\tilde{\boldsymbol{\omega}}_t - \mathbf{b}_t^g - \mathbf{w}_t^g)^\wedge\left(\mathbf{I}_{3\times3} + \left(\boldsymbol{\xi}_t^R\right)^\wedge\right)\\ &+ \left(\mathbf{I}_{3\times3} + \left(\boldsymbol{\xi}_t^R\right)^\wedge\right)(\tilde{\boldsymbol{\omega}}_t - \hat{\mathbf{b}}_t^g)^\wedge\\ &= (\mathbf{b}_t^g - \hat{\mathbf{b}}_t^g + \mathbf{w}_t^g)^\wedge - (\tilde{\boldsymbol{\omega}}_t - \mathbf{b}_t^g - \mathbf{w}_t^g)^\wedge\left(\boldsymbol{\xi}_t^R\right)^\wedge\\ &+ \left(\boldsymbol{\xi}_t^R\right)^\wedge(\tilde{\boldsymbol{\omega}}_t - \mathbf{b}_t^g)^\wedge\\ &= (-\boldsymbol{\zeta}_t^g + \mathbf{w}_t^g)^\wedge - (\tilde{\boldsymbol{\omega}}_t - \boldsymbol{\zeta}_t^g)^\wedge(\boldsymbol{\xi}_t^R)^\wedge + (\boldsymbol{\xi}_t^R)^\wedge(\tilde{\boldsymbol{\omega}}_t - \boldsymbol{\zeta}_t^g)^\wedge\\ &+ (\mathbf{b}_t^g - \hat{\mathbf{b}_t^g})^\wedge(\boldsymbol{\xi}_t^R)^\wedge\\ &= \left(-(\tilde{\boldsymbol{\omega}}_t - \boldsymbol{\zeta}_t^g)^\wedge\boldsymbol{\xi}_t^R - \boldsymbol{\zeta}_t^g + \mathbf{w}_t^g\right)^\wedge\\ &- \left((\mathbf{b}_t^g)^\wedge\boldsymbol{\xi}_t^R\right)^\wedge - (\boldsymbol{\zeta}_t^g)^\wedge(\boldsymbol{\xi}_t^R)^\wedge\\ &\approx \left((-\tilde{\boldsymbol{\omega}}_t)^\wedge\boldsymbol{\xi}_t^R - \boldsymbol{\zeta}_t^g + \mathbf{w}_t^g\right)^\wedge\end{aligned}$$

where the last line is derived by only keeping the first order term. Similar to the derivation above, we developed the rest of the error terms as follows

$$\frac{d}{dt}\left(\mathbf{R}_t^T(\hat{\mathbf{v}}_t - \mathbf{v}_t)\right) = -(\tilde{\mathbf{a}}_t)^\wedge\boldsymbol{\xi}_t^R - (\tilde{\boldsymbol{\omega}}_t)^\wedge\boldsymbol{\xi}_t^v - \boldsymbol{\zeta}_t^a + \mathbf{w}_t^a$$
$$\frac{d}{dt}\left(\mathbf{R}_t^T(\hat{\mathbf{p}}_t - \mathbf{p}_t)\right) = \boldsymbol{\xi}_t^v - (\tilde{\boldsymbol{\omega}}_t)^\wedge\boldsymbol{\xi}_t^p$$

Define the augmented error as follows,

$$\mathbf{w}_t = vec(\mathbf{w}_t^g, \mathbf{w}_t^a, \mathbf{0}_{3\times1}, \mathbf{w}_t^{tg}, \mathbf{w}_t^{ba}) \tag{63}$$

By definition of the left invariant error, it follows that

$$\begin{aligned}\frac{d}{dt}\boldsymbol{\eta}_t^l &= \mathcal{L}_{\mathfrak{g}}\left(\begin{bmatrix}\frac{d}{dt}(\mathbf{R}_t^{-1}\hat{\mathbf{R}}_t)\\ \frac{d}{dt}(\mathbf{R}_t^{-1}\hat{\mathbf{v}}_t - \mathbf{R}_t^{-1}\mathbf{v}_t)\\ \frac{d}{dt}(\mathbf{R}_t^{-1}\hat{\mathbf{p}}_t - \mathbf{R}_t^{-1}\mathbf{p}_t)\end{bmatrix}\right)\\ &= \mathcal{L}_{\mathfrak{g}}\left(\begin{bmatrix}-(\tilde{\boldsymbol{\omega}}_t)^\wedge\boldsymbol{\xi}_t^g - \boldsymbol{\zeta}_t^g + \mathbf{w}_t^g\\ -(\tilde{\mathbf{a}}_t)^\wedge\boldsymbol{\xi}_t^g - (\tilde{\boldsymbol{\omega}}_t)^\wedge - \boldsymbol{\zeta}_t^a + \mathbf{w}_t^a\\ \boldsymbol{\xi}_t^v - (\tilde{\boldsymbol{\omega}}_t)^\wedge\boldsymbol{\xi}_t^p\end{bmatrix}\right)\\ &= \mathcal{L}_{\mathfrak{g}}(\mathbf{A}_t^l\mathbf{e}_t^l + \mathbf{w}_t)\end{aligned}$$

Decompose the vector into $\mathbf{A}_t^l$ and the invariant error $\mathbf{e}_t^l$.

$$\mathbf{A}_t^l = \begin{bmatrix}-(\tilde{\boldsymbol{\omega}}_t)^\wedge & \mathbf{0} & \mathbf{0} & -\mathbf{I} & \mathbf{0}\\ -(\tilde{\mathbf{a}}_t)^\wedge & -(\tilde{\boldsymbol{\omega}}_t)^\wedge & \mathbf{0} & \mathbf{0} & -\mathbf{I}\\ \mathbf{0} & \mathbf{I} & -(\tilde{\boldsymbol{\omega}}_t)^\wedge & \mathbf{0} & \mathbf{0}\\ \mathbf{0} & \mathbf{0} & \mathbf{0} & \mathbf{0} & \mathbf{0}\\ \mathbf{0} & \mathbf{0} & \mathbf{0} & \mathbf{0} & \mathbf{0}\end{bmatrix}$$

C. Discretization and Prediction

Using the results derived above, we can describe the prediction step of LI-EKF with IMU bias in terms of the state estimate $\hat{\mathbf{X}}_t$ and the augmented covariance matrix $\mathbf{P}_t$:

$$\frac{d}{dt}\hat{\mathbf{X}}_t = f_{\mathbf{u}_t,\boldsymbol{\theta}_t}(\hat{\mathbf{X}}_t), \frac{d}{dt}\mathbf{P}_t = \mathbf{A}_t^l\mathbf{P}_t + \mathbf{P}_t\mathbf{A}_t^l + \hat{\mathbf{Q}}_t$$

where $\hat{\mathbf{Q}}_t = \text{Cov}(\mathbf{w}(t))$. For implementation purpose, the continuous-time dynamics derived earlier is converted into discrete-time models using zero-order hold euler integration as follows,

$$\hat{\mathbf{R}}_{t_k} = \mathbf{R}_{t_{k-1}} exp((\tilde{\boldsymbol{\omega}}_t - \hat{\mathbf{b}}_t^g)\Delta t) \tag{64}$$

$$\hat{\mathbf{v}}_{t_k} = \mathbf{v}_{t_{k-1}} + (\mathbf{R}_{t_{k-1}}(\tilde{\mathbf{a}}_t - \hat{\mathbf{b}}_t^a) + \mathbf{g})\Delta t \tag{65}$$

$$\hat{\mathbf{p}}_{t_k} = \mathbf{p}_{t_{k-1}} + \mathbf{v}_{t_{k-1}}\Delta t + \frac{1}{2}(\mathbf{R}_{t_{k-1}}(\tilde{\mathbf{a}}_t - \hat{\mathbf{b}}_t^a) + \mathbf{g})\Delta t^2 \tag{66}$$

The discrete time IMU bias estimates are propogated through their deterministic dynamics,

$$\hat{\mathbf{b}}_{t_k}^g = \hat{\mathbf{b}}_{t_{k-1}}^g, \hat{\mathbf{b}}_{t_k}^a = \hat{\mathbf{b}}_{t_{k-1}}^a$$

Combining the state and IMU bias, the discrete-time covariance propogation under zero-order hold Euler integration can be described as:

$$\mathbf{P}_{t_k} = \boldsymbol{\Phi}\mathbf{P}_{t_{k-1}}\boldsymbol{\Phi}^T + \boldsymbol{\Phi}Q_{t_{k-1}}\boldsymbol{\Phi}^T\Delta t$$

where $\boldsymbol{\Phi} = \text{expm}(\mathbf{A}_t^l\Delta t)$.

D. Correction with GPS measurement

Since the measurement (GPS signal) is not correlated with the IMU bias, the correction step will be in the same formulation as developed in Section III. Note that in discrete time models, IMU bias state $\boldsymbol{\theta}_t$ are propagated along with the original state matrix. For simplification, we define the augmented state matrix $\hat{\mathbf{X}}_{k,aug}$ as:

$$\hat{\mathbf{X}}_{k,aug} = \begin{bmatrix} \hat{\mathbf{R}}_k & \hat{\mathbf{v}}_k & \hat{\mathbf{p}}_k & \hat{\mathbf{b}}_k^g & \hat{\mathbf{b}}_k^a \\ \mathbf{0}_{1\times3} & 1 & 0 & 0 & 0 \\ \mathbf{0}_{1\times3} & 0 & 1 & 0 & 0 \\ \mathbf{0}_{1\times3} & 0 & 0 & 1 & 0 \\ \mathbf{0}_{1\times3} & 1 & 0 & 0 & 1 \end{bmatrix}$$

The measurement model is modified with original matrices augmented accordingly,

$$\begin{aligned} \mathbf{Y}_{k,aug} &= \hat{\mathbf{X}}_{k,aug}\mathbf{b}_{aug} + \mathbf{V}_{k,aug} \\ &= [\mathbf{y}_k, 0, 1, 0, 0]^T \\ \mathbf{b}_{aug} &= [\mathbf{0}_{3\times1}, 0, 1, 0, 0]^T \\ \mathbf{V}_{k,aug} &= [\mathbf{v}_k, 0, 0, 0, 0]^T \end{aligned}$$

The measurement Jacobian should be augmented with 0 since measurement is not dependent on the additional states (IMU bias):

$$\mathbf{H} = \begin{bmatrix} \mathbf{0}_{3\times3} & \mathbf{0}_{3\times3} & \mathbf{I}_{3\times3} & \mathbf{0}_{3\times3} & \mathbf{0}_{3\times3} \end{bmatrix}$$

Using these augmented matrices and augmented state matrix, the final equations for correction step are summarized as follows:

$$\hat{\mathbf{X}}_{k,aug}^+ = \hat{\mathbf{X}}_{k,aug}\text{exp}\left(\mathbf{L}_{t_k}\left(\hat{\mathbf{X}}_{k,aug}^{-1}\mathbf{Y}_{k,aug} - \mathbf{b}\right)\right) \tag{67}$$

$$\mathbf{P}_k^+ = (\mathbf{I} - \mathbf{L}_k\mathbf{H})\mathbf{P}_k(\mathbf{I} - \mathbf{L}_k\mathbf{H})^T + \mathbf{L}_k\hat{\mathbf{N}}_k\mathbf{L}_k^T, \tag{68}$$

where

$$\begin{aligned} \hat{\mathbf{N}}_k &= \hat{\mathbf{X}}_{k,aug}^{-1}\text{Cov}[\mathbf{V}_{k,aug}]\hat{\mathbf{X}}_{k,aug}^{-T}, \\ \mathbf{L}_k &= \mathbf{P}_k\mathbf{H}^T\mathbf{S}^{-1}, \\ \mathbf{S} &= \mathbf{H}\mathbf{P}_k\mathbf{H}^T + \hat{\mathbf{N}}_k \end{aligned}$$

V. EXTENDED KALMAN FILTER

In this section we present the EKF which we use to compare the results of our LI-EKF against.

A. State Representation

Similar to [4], we present our state space representation of the model with Orientation, Velocity and Position of the robot in the world frame. Specifically, $\mathbf{X}_t \in R^9$ is given by:

$$\mathbf{X}_t = (\mathbf{O}_t, \mathbf{v}_t, \mathbf{p}_t)^T \tag{69}$$

where $\mathbf{O}_t = (\phi_k, \theta_k, \psi_k)^T$ is the estimated orientation in euler angles, $\mathbf{v}_t = (\dot{x}_k, \dot{y}_k, \dot{z}_k)^T$ is the velocity and $\mathbf{p}_t = (x_k, y_k, z_k)^T$ is the position of the robot in the world frame.

B. System Dynamics

Given the angular velocity ω_t and acceleration a_t measurements from the IMU, the orientation (given in quaternions) is estimated using the Madgwick Filter as described in [3].

Velocity and Position are propagated as follows:

$$\mathbf{X}_t(4:9) = \begin{bmatrix} \mathbf{V}_k \\ \mathbf{P}_k \end{bmatrix} = \begin{bmatrix} \mathbf{I} & 0 \\ \mathbf{I} * \mathbf{T}_s & \mathbf{I} \end{bmatrix}\mathbf{X}_{t-1}(4:9) + \begin{bmatrix} \mathbf{T}_s * \mathbf{I} \\ \mathbf{T}_s^2/2 * \mathbf{I} \end{bmatrix} a_{t-1}^W \tag{70}$$

Here, a_{t-1}^W is the acceleration of the robot in the world frame and is given by

$$a_t^W = \mathbf{Q}_t * a_t^B * \mathbf{Q}_t' - G \tag{71}$$

where $*$ is the quaternion multiplication. $G = (0, 0, g)^T$ is earth's gravity and $\mathbf{Q}_t = (q_{w,t}, q_{1,t}, q_{2,t}, q_{3,t})^T$ is the quaternion representation of the rotation transformation between the inertial sensor frame $\mathbf{B}$ and the global reference frame $\mathbf{W}$.

The discretized model is given by

$$\mathbf{X}_t = \begin{bmatrix} \mathbf{O}_k \\ \mathbf{V}_k \\ \mathbf{P}_k \end{bmatrix} = \underbrace{\begin{bmatrix} 0 & 0 & 0 \\ 0 & \mathbf{I} & 0 \\ 0 & dt * \mathbf{I} & \mathbf{I} \end{bmatrix}}_{\text{A}}\mathbf{X}_{t-1} + \underbrace{\begin{bmatrix} \mathbf{T}_s^2/2 * \mathbf{I} \\ \mathbf{T}_s * \mathbf{I} \\ 0 \end{bmatrix}}_{\text{B}} a_{t-1}^W + \begin{bmatrix} Q2Euler(\mathbf{Q}_t) \\ 0 \\ 0 \end{bmatrix} + w_t \tag{72}$$

Here, the $Q2Euler(\mathbf{Q}_t)$ is a function to transform the quaternion orientation obtained from the madgwick filter for propagating the orientation. w_t is the process noise with noise covariance matrix given by $\mathbf{W}_t$. The state covariance is propogated using the following equation:

$$\mathbf{\Sigma_t^-} = A\mathbf{\Sigma_t}A^T + \mathbf{W}_t \tag{73}$$

C. Measurement model

Similar to the In-EKF, the measurements taken are the positions x and y from the latitude and longitude measurements of the GPS.

$$z_t = \mathbf{H}\mathbf{X}_t^- + n_t \tag{74}$$

where n_k is the measurement noise given by the noise covariance matrix $\mathbf{R}_t$ and $\mathbf{H}$ is given by

$$\mathbf{H} = \begin{bmatrix} 0 & 0 & 0 & 0 & 0 & 0 & 1 & 0 & 0 \\ 0 & 0 & 0 & 0 & 0 & 0 & 0 & 1 & 0 \end{bmatrix} \tag{75}$$

The innovation v_t is given by

$$v_t = z_t - \mathbf{H}\mathbf{X}_t^- \tag{76}$$

and the filter gain $\mathbf{K}$ is given by

$$\mathbf{S}_t = \mathbf{H}\mathbf{\Sigma_t^-}\mathbf{H}^T + \mathbf{R}_t \tag{77}$$

$$\mathbf{K}_t = \mathbf{\Sigma_t^-}\mathbf{H}^T\mathbf{S}_t^{-1} \tag{78}$$

The corrected state and the state covaraince is given by

$$\mathbf{X}_t = \mathbf{X}_t^- + \mathbf{K}_t v_t \tag{79}$$

$$\mathbf{\Sigma_t} = (\mathbf{I} - \mathbf{K}_t\mathbf{H}_t)\mathbf{\Sigma_t^-}(\mathbf{I} - \mathbf{K}_t\mathbf{H}_t)^T + \mathbf{K}_t\mathbf{R}_t\mathbf{K}_t^T \tag{80}$$

VI. RESULTS

The filters were tested using the NCLT dataset [20] containing IMU and GPS data. Sensors used for navigation relative to this project are an Microstrain 3DM-GX3-45 IMU (3-axis accelerometers, gyroscopes, and magnetometers) and a Garmin 18x 5Hz consumer grade GPS. The dataset also preprocessed a large SLAM solution with all sessions using lidar scan matching and high-accuracy RTK GPS to provide ground-truth robot pose. Data recorded on 2013-01-10 were used in this project. Fig. 1 shows the overall robot trajectory overlaid onto Google Maps based on pure GPS data.

The proposed Left-invariant EKF without IMU bais was first implemented to investigate potential benefits or drawbacks of the filter. The noise statistics and initial covariance estimates are provided in Table I. The euler angle estimates as well as their corresponding ground-truth are shown in Fig. 2. As shown in the figure, solid lines (LI-EKF estimates) follow the trend of dashed lines (ground-truth) pretty well. Roll and pitch angles are correctly estimated by the filter as small angles close to 0 since the robot is moving smoothly on the horizontal plane. However, clearly, there is an ever-growing offset between the estimated yaw angle and the ground-truth, which can be attributed to lack of gyro bias in the modeling. Fig. 3 shows x, y, θ, ψ estimate errors as well as their 3-sigma contours for the LI-EKF filter. Conclusion can be drawn from the figure that robot pose can be accurately extracted from the LI-EKF filter except that some extra modeling of the gyro yaw angle (adding gyro bias) is needed.

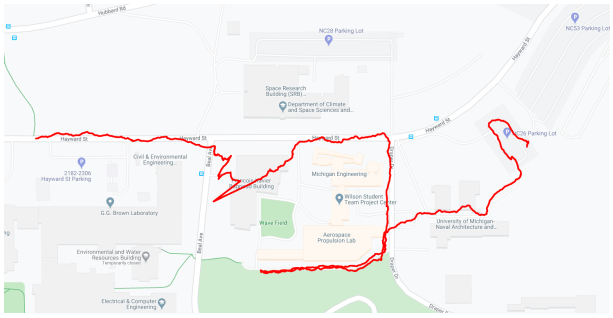

Fig. 1. Robot Trajectory Overlaid onto Google Maps

TABLE I
EXPERIMENT NOISE STATISTICS AND INITIAL COVARIANCE

State Element / Measurement Type	noise st. dev.
Lie algebra $\boldsymbol{\xi}$	eye(9)
Accelerometer Noise	0.014 m/sec^2
Gyroscope Noise	0.01 rad/sec
GPS Noise	1 m

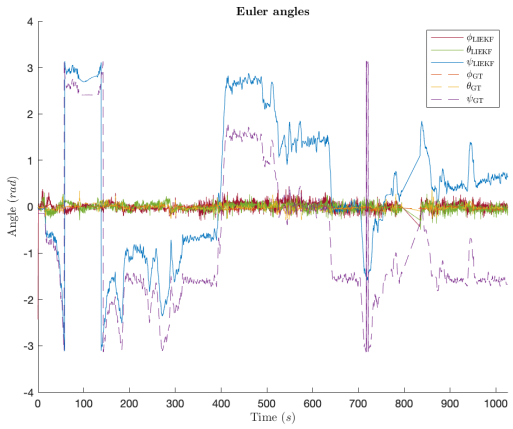

Fig. 2. Euler Angle plots for LiEKF

Similar to the In-EKF, the Euler Angle estimates as well as their corresponding ground-truths are shown in Fig. 4. This plot is very similar to the In-EKF and the differences only noticeable upon closer inspection. Fig. 5 shows x, y, θ, ψ estimate errors and the 3-sigma contours for the EKF filter. Here, it can be seen that x and y go out of the sigma bounds which is a weaker performance compared to the In-EKF. Fig. 6 and Fig. 7 show the trajectories obtained by running through the EKF and In-EKF respectively and as can be seen they are quite close.

We also made attempts to add imu bias to the LI-EKF based on the implemented Left-invariant EKF program. Following the derivation in Section V, the modified prediction model augments the original state matrix to include IMU bias states. The augmented state matrix is then propagated

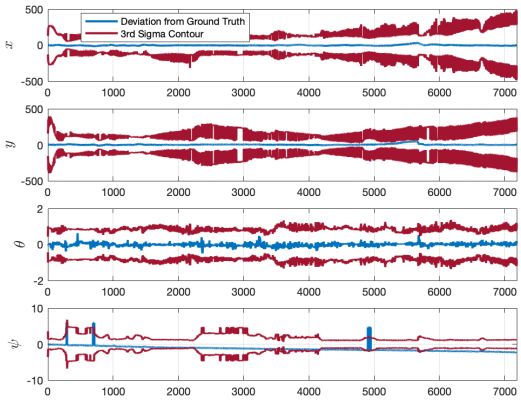

Fig. 3. Error plots for LiEKF

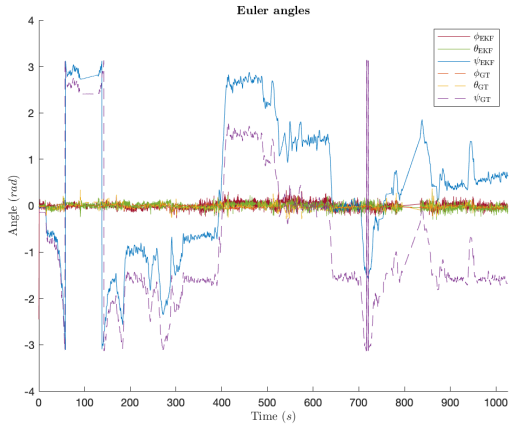

Fig. 4. Euler Angle plots for EKF

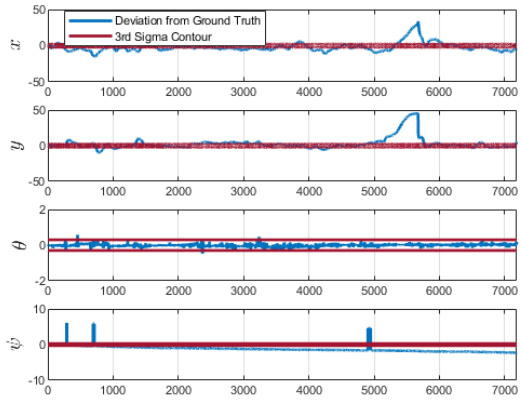

Fig. 5. Error plots for EKF

through deterministic dynamics, and then updated by GPS measurement correction with matrices augmented accordingly. A trajectory is successfully generated by the LI-EKF filter including IMU bias, which is close to the one LI-EKF without IMU bias generated when plotted together for comparison. However, there is a lot of discrepancy between the euler angle estimated by LI-EKF with bias and

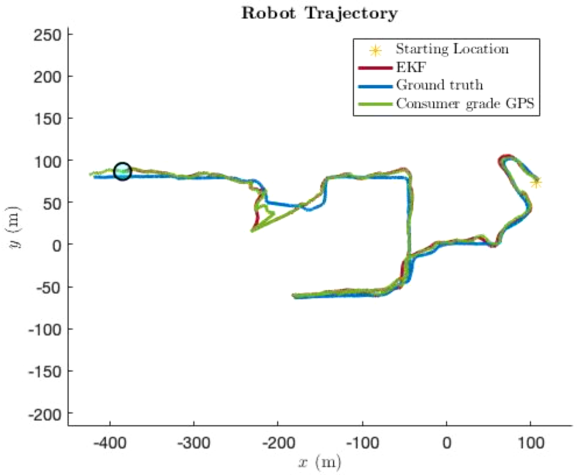

Fig. 6. Predicted robot trajectory using EKF

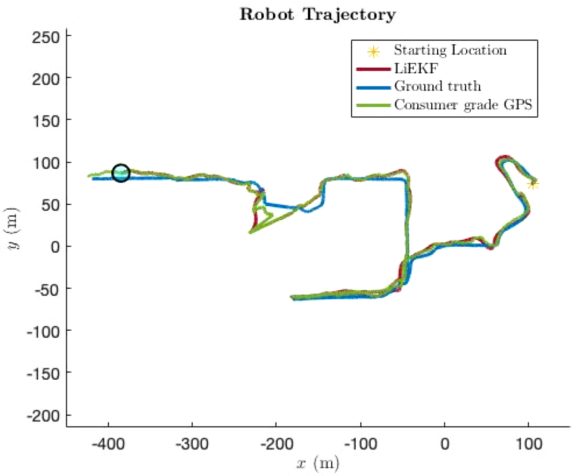

Fig. 7. Predicted robot trajectory using LiEKF

the ground truth. Unfortunately, despite various approaches attempted, due to the time limit we are unable to resolve this issue in our implementation.

VII. CONCLUSIONS

In this final project, we've successfully reimplemented two filter based localization algorithms namely EKF and LI-EKF. We applied such methods onto the North Campus Long Term Vision Dataset to localize a mobile robot travelling across the North Campus. We demonstrated that these methods are able to very accurately track the robot's trajectory over time. In addition, we also attempted to integrate IMU biases into the LiEKF algorithm to achieve better performance. For future works, we hope to complete and fully test our integration of IMU biases as well as evaluate our method on other datasets.

ACKNOWLEDGMENT

The authors would like thank Maani Ghaffari Jadidi for his excellent lectures and valuable homework projects to enhance our understanding of the SLAM technology.

REFERENCES

[1] B. Barshan and H. F. Durrant-Whyte, *Inertial navigation systems for mobile robots*, vol. 11, pp. 328–342, June 1995.

[2] D. H. Titterton and J. L. Weston, *Strapdown inertial navigation technology*. The Institution of Electrical Engineers, 2004.

[3] H. J. Luinge and P. H. Veltink, *Inclination measurement of human movement using a 3-d accelerometer with autocalibration*, vol. 12, pp. 112–121, Mar. 2004.

[4] H. Zhou and H. Hu, *Human motion tracking for rehabilitation - a survey*, Biomedical Signal Processing and Control, vol. 3, no. 1, pp. 1-18, 2008.

[5] E. A. Heinz, K. S. Kunze, M. Gruber, D. Bannach, and P. Lukowicz, *Using wearable sensors for real-time recognition tasks in games of martial arts - an initial experiment*, in Proc. IEEE Symposium on Computational Intelligence and Games, pp. 98–102, May 22–24, 2006.

[6] Q. Tong, P. Li, and S. Shen. *Vins-mono: A robust and versatile monocular visual-inertial state estimator*. IEEE Transactions on Robotics 34.4 (2018): 1004-1020.

[7] C. Forster, L. Carlone, F. Dellaert, and D. Scaramuzza, *IMU preintegration on manifold for efficient visual-inertial maximum-a-posteriori estimation*. Georgia Institute of Technology, 2015.

[8] S. Leutenegger, S. Lynen, M. Bosse, R. Siegwart, and P. Furgale, *Keyframe-based visual-inertial odometry using nonlinear optimization*, Int. J. Robot. Research, vol. 34, no. 3, pp. 314–334, Mar. 2014.

[9] A. I. Mourikis and S. I. Roumeliotis, *A multi-state constraint Kalman filter for vision-aided inertial navigation*, in Proc. of the IEEE Int. Conf. on Robot. and Autom., Roma, Italy, Apr. 2007, pp. 3565–3572.

[10] M. Li and A. Mourikis, *High-precision, consistent EKF-based visual-inertial odometry*, Int. J. Robot. Research, vol. 32, no. 6, pp. 690–711, May 2013.

[11] M. Bloesch, S. Omari, M. Hutter, and R. Siegwart, *Robust visual inertial odometry using a direct ekf-based approach*, in Proc. of the IEEE/RSJ Int. Conf. on Intell. Robots and Syst. IEEE, 2015, pp. 298-304.

[12] A. Barrau and S. Bonnabel, *Invariant Kalman filtering*, in Annual Review of Control, Robotics, and Autonomous Systems, 2018.

[13] S. Bonnabel, P. Martin, and P. Rouchon. *Nonlinear symmetry-preserving observers on Lie groups*, in IEEE Transactions on Automatic Control, 54(7):1709–1713, 2009.

[14] A. Barrau. *Non-linear state error based extended Kalman filters with applications to navigation*. PhD thesis, Mines Paristech, 2015.

[15] A. Barrau and S. Bonnabel. *The invariant extended Kalman filter as a stable observer*. IEEE Transactions on Automatic Control, 62(4):1797–1812, 2017.

[16] T. Zhang, K. Wu, J. Song, S. Huang, and G. Dissanayake. *Convergence and consistency analysis for a 3-D invariant-EKF SLAM*. IEEE Robotics and Automation Letters, 2(2):733–740, 2017.

[17] M. Barczyk and A. Lynch. *Invariant observer design for a helicopter UAV aided inertial navigation system*. IEEE Transactions on Control Systems Technology, 21(3):791–806, 2013.

[18] R. Hartley, M. Ghaffari, J. Grizzle, and R. Eustice, *Contact-aided invariant extended Kalman filtering for legged robot state estimation*, arXiv preprint arXiv:1805.10410, 2018.

[19] R. Hartley, M. Ghaffari, R. Eustice, and J. Grizzle, *Contact-aided invariant extended Kalman filtering for robot state estimation*. The International Journal of Robotics Research, 39(4), 402-430, 2020.

[20] N. Carlevaris, A. Ushani, and R. Eustice, *University of Michigan North Campus long-term vision and lidar dataset*. International Journal of Robotics Research, 35(9):1023-1035, 2015.

[21] B. Hall. *Lie groups, Lie algebras, and representations: an elementary introduction*, volume 222. Springer, 2015.

[22] S. O. H. Madgwick, A. J. L. Harrison and R. Vaidyanathan, *Estimation of IMU and MARG orientation using a gradient descent algorithm* 2011 IEEE International Conference on Rehabilitation Robotics, Zurich, 2011, pp. 1-7.